Integrative Biology

RSC Publishing

PAPER

View Article Online
View Journal

Cite this: DOI: 10.1039/c3ib40027a

Molecular mechanisms of biomaterial-driven osteogenic differentiation in human mesenchymal stromal cells†

Ana M. C. Barradas,[a] Veronica Monticone,[a] Marc Hulsman,[b] Charlène Danoux,[a] Hugo Fernandes,[a] Zeinab Tahmasebi Birgani,[a] Florence Barrère-de Groot,[c] Huipin Yuan,[ac] Marcel Reinders,[b] Pamela Habibovic,[a] Clemens van Blitterswijk[a] and Jan de Boer*[a]

Calcium phosphate (CaP) based ceramics are used as bone graft substitutes in the treatment of bone defects. The physico-chemical properties of these materials determine their bioactivity, meaning that molecular and cellular responses in the body will be tuned accordingly. In a previous study, we compared two porous CaP ceramics, hydroxyapatite (HA) and β-tricalcium phosphate (TCP), which, among other properties, differ in their degradation behaviour *in vitro* and *in vivo*, and we demonstrated that the more degradable β-TCP induced more bone formation in a heterotopic model in sheep. This is correlated to *in vitro* data, where human bone marrow derived mesenchymal stromal cells (MSC) exhibited higher expression of osteogenic differentiation markers, such as osteopontin, osteocalcin and bone sialoprotein, when cultured in β-TCP than in HA. More recently, we also showed that this effect could be mimicked *in vitro* by exposure of MSC to high concentrations of calcium ions (Ca^{2+}). To further correlate surface physico-chemical dynamics of HA and β-TCP ceramics with the molecular response of MSC, we followed Ca^{2+} release and surface changes in time as well as cell attachment and osteogenic differentiation of MSC on these ceramics. Within 24 hours, we observed differences in cell morphology, with MSC cultured in β-TCP displaying more pronounced attachment and spreading than cells cultured in HA. In the same time frame, β-TCP induced expression of G-protein coupled receptor (GPCR) 5A and regulator of G-protein signaling 2, revealed by DNA microarray analysis. These genes, associated with the protein kinase A and GPCR signaling pathways, may herald the earliest response of MSC to bone-inducing ceramics.

Received 4th February 2013,
Accepted 18th April 2013

DOI: 10.1039/c3ib40027a

www.rsc.org/ibiology

Insight, innovation, integration

β-Tricalcium phosphate (β-TCP) and hydroxyapatite (HA), two calcium phosphate ceramics, were previously shown to induce bone formation in the muscle of dogs (after implantation without cells). β-TCP yielded more bone than HA, making it a promising bone graft substitute. Using an *in vitro* model, here we compared the early biological response of human mesenchymal stromal cells to these ceramics. We identified a set of genes upregulated by β-TCP compared to HA and further correlated that with the physico-chemical properties of the ceramics, where calcium ions are expected to play a role. This model may allow us to understand the complex *in vivo* mechanism that leads to such discrepant bone formation outcomes, allowing us to design more efficient biomaterials.

[a] *Department of Tissue Regeneration, MIRA Institute for Biomedical Technology and Technical Medicine, University of Twente, Drienerlolaan 5, 7522 NB Enschede, The Netherlands. E-mail: anabarradas@me.com, vemo87@gmail.com, c.b.s.s.danoux@utwente.nl, h.a.m.fernandes@utwente.nl, Z.Tahmasebi@utwente.nl, p.habibovic@utwente.nl, c.a.vanblitterswijk@tnw.utwente.nl, j.deboer@utwente.nl; Fax: +31 (0)53 489 2150; Tel: +31 (0)53 489 3400*

[b] *Delft Bioinformatics Lab, Delft University of Technology, Mekelweg 4, 2628 CD Delft, The Netherlands. E-mail: m.hulsman@tudelft.nl, M.J.T.Reinders@tudelft.nl; Fax: +31 (0)15 27 81843; Tel: +31 (0)15 27 86052*

[c] *Xpand Biotechnology BV, Bilthoven, The Netherlands. E-mail: florence.de.groot@xpand-biotech.com, huipin.yuan@xpand-biotech.com; Fax: +31 (0)30 229 7299; Tel: +31 (0)30 229 7280*

† Electronic supplementary information (ESI) available. See DOI: 10.1039/c3ib40027a

Introduction

In the occurrence of a bone defect due to trauma or tumor resection, bone void fillers are needed to regain the bone's original properties and functions. Autologous bone grafting (autograft), in which healthy bone is collected and transplanted to the defect, is the most frequently applied therapy in such situations. Autografts are osteoinductive (*i.e.* they induce commitment of undifferentiated cells to become osteoblasts) and osteoconductive (*i.e.* provide a framework for bone ingrowth), two properties that determine successful bone regeneration. However, the amount of bone that can be collected is limited, and furthermore, the method may pose severe disadvantages, such as donor-site pain and morbidity.[1] Due to these limitations, and concomitant with an increasing world population, there is an urgent demand for bone graft substitutes (BGS).[2]

Among BGS, synthetic calcium phosphate (CaP) ceramics are widely used because their chemical composition resembles that of bone mineral.[3–5] Besides, the majority of CaP ceramics are osteoconductive, providing excellent osteointegration between the host bone and the implant. Ideally, CaP BGS should also possess intrinsic osteoinductivity, however only a sub-class of these materials has been shown osteoinductive, as demonstrated by *de novo* bone formation upon heterotopic implantation, for example in muscle (without cells or growth factors) in pre-clinical animal models.[6,7]

In the past few decades, several formulations of CaP ceramics have been developed that vary, in terms of chemical composition, in crystallinity and macro- and micro-scaled structural features. In general, most formulations include macro-scaled pores, which are void spaces in the structure that allow ingrowth of cells, blood vessels and tissue, and some contain micro-scaled pores as well (defined as having a diameter smaller than 10 μm). Chemical composition of the material is often characterised by the calcium to phosphate ratio (Ca/P). In general, lower Ca/P ratios lead to a higher dissolution rate. For instance, hydroxyapatite (HA), with a Ca/P ratio of 1.67, dissolves slower than tricalcium phosphate (TCP), whose Ca/P ratio is 1.5.[8,9] However, all above mentioned properties, together with mechanical properties and the presence of cells, such as osteoclasts, can affect CaP degradability.

So far, there has been no clear link between the physico-chemical properties of CaP BGS and their bioactivity at the molecular level. Further impairing such knowledge is the fact that a stringent comparison between different studies and labs cannot be done. Although a material might bear the same name in different publications, usually following its chemical composition, other properties can be different due to the protocols used for its preparation. Nonetheless, a fundamental understanding of the physico-chemical properties of a particular set of materials that drive specific molecular and cellular responses might improve the design of CaP biomaterials and perhaps unlock other clinical therapies for bone regeneration, not considered so far.

Within limits, *in vitro* models can help understanding how CaP ceramics regulate osteogenic differentiation of cells. As such, CaP based materials and their bioactivity in terms of osteogenic differentiation (*in vitro*), and in some cases, correlation with bone-forming capacity (*in vivo*) have been a subject of intensive research. For instance, Matsushima and colleagues[10] observed that bone marrow-derived mesenchymal stromal cells (MSC) combined with β-TCP formed more bone in a subcutaneous *in vivo* model in nude rats, than MSC grown on HA. Although in both cases MSC were alkaline phosphatase (ALP) positive *in vitro* prior to implantation, there was no quantitative analysis of ALP staining. Tan *et al.*[11] also observed that HA and biphasic calcium phosphate (BCP) induced expression of osteogenic markers in C2C12 cells but did not quantify the differences between the two ceramics. SaOS-2 cells showed higher levels of ALP activity when cultured in HA (Osbone®) granules than when cultured in β-TCP (Cerasorb®) but differences between the two ceramics in gene expression of typical osteogenic differentiation markers, such as osteopontin (OP), bone sialoprotein (BSP) and osteonectin (ON), were not observed.[12] Similarly, HA also induced higher levels of ALP gene expression in SaOS-2 cells than BCP or TCP did, but no statistically significant differences were detected regarding expression of OC, ON and collagen type I (Col I).[13]

In contrast, we showed that MSC cultured in β-TCP did express more OP, OC, Col I and BSP than in HA after 7 days. In addition we also showed that β-TCP, without cells, induced 5 times more bone formation than HA, when implanted intramuscularly in dogs (osteoinduction),[14] further correlating *in vivo* bone forming capacity and osteogenic differentiation potential *in vitro*.

Since β-TCP and HA used in our study showed clear differences in *in vitro* dissolution rates, we hypothesized that calcium ion (Ca^{2+}) dissolution is a factor driving MSC osteogenic differentiation *in vitro* and bone formation *in vivo*. More recently, we actually demonstrated that indeed MSC express more OP, OC, BSP and in addition more BMP-2 in a high Ca^{2+} concentration ([Ca^{2+}]) milieu than in a low one,[15] in accordance with the osteogenic profile of cell selected by β-TCP (higher solubility) and HA (lower solubility).[14]

In this study, we used MSC to investigate the biological mechanism that leads to such distinct osteoblastic phenotypes on β-TCP *versus* HA. We analysed MSC gene expression differences at very early time points through DNA microarray analysis. Also, we further characterized physico-chemical properties of these ceramics associated with their dissolution/precipitation surface events.

Materials and methods

HA and β-TCP fabrication

HA ceramics were prepared from HA powder (Merck) using the dual-phase mixing method and sintered at 1250 °C for 8 hours, according to a previously described method.[16] β-TCP ceramics were prepared from TCP powder (Plasma Biotal) and sintered at 1100 °C. Ceramic particles were cleaned ultrasonically with acetone, 70% ethanol and demineralized water and dried at 80 °C. Particles were sieved to obtain a 1–2 mm sized particle

batch, and were autoclaved prior to use. For a detailed physicochemical characterization of these materials the reader is referred to Yuan *et al.*[14]

Inductively coupled plasma-optical emission spectrometry

In a previous study, we showed the Ca^{2+} release profile from HA and β-TCP in simulated physiological saline (SPS) for approximately 3 hours.[14] Here, we studied the release profiles of Ca^{2+} and PO_4^{3-}, on a time scale corresponding to cell culturing experiments (days). Fifteen particles of either HA or β-TCP were immersed in 10 ml of either simulated physiological saline (SPS; 0.8% NaCl, 50 mM HEPES, pH 7.3) or minimum essential medium α (α-MEM, Gibco) for four hours, then solutions were refreshed with 500 μl of respective liquid and after four hours, refreshed again, but this time, with 10 ml. All incubation steps were carried out in a 5% CO_2 humid atmosphere at 37 °C, according to what is usually done in cell culture experiments: ceramics pre-wetting for 4 hours, followed by cell seeding in low volume and then addition of cell culture medium. For a schematic representation of procedures see Fig. 1A.

At specific time points, SPS and α-MEM samples were collected for $[Ca^{2+}]$ and $[PO_4^{3-}]$ measurements using Inductively Coupled Plasma-Optical Emission Spectrometry (ICP-OES, Varian 720 ES, Evisa). Standard samples for Ca^{2+} and PO_4^{3-} measurements were prepared by dissolving $CaCl_2{\cdot}2H_2O$ and $Na_2HPO_4{\cdot}2H_2O$, respectively, in SPS solution with varying concentrations. Individual samples were prepared for each time point collection, to ensure that concentrations would not be disturbed by incomplete liquid removal for analysis. Each data point represents one measurement ($n = 1$). Due to the technical difficulties associated with ICP-OES analysis, we did not add FBS to α-MEM, which is usually present at a concentration of 10%. It should be noted that SPS does not contain Ca^{2+} or PO_4^{3-}, whereas α-MEM contains 1.8 mM $CaCl_2$ and 1.01 mM NaH_2PO_4.

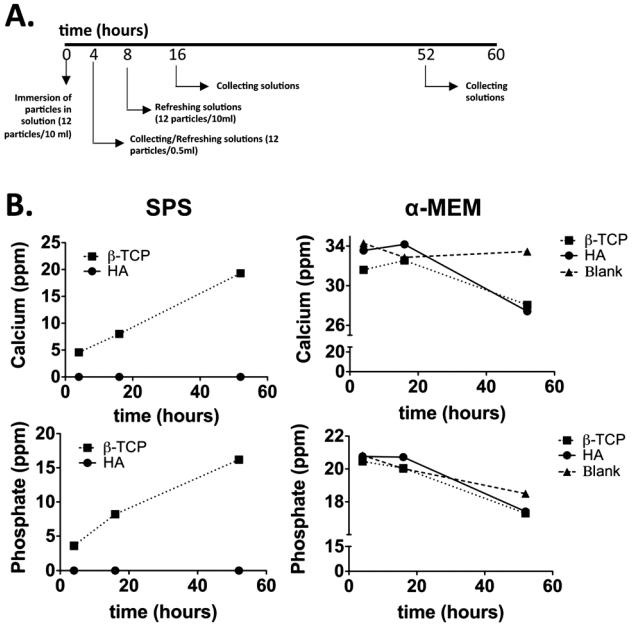

Fig. 1 Ca^{2+} and PO_4^{3-} dissolution from HA and β-TCP into SPS and α-MEM. (A) HA and β-TCP particles were incubated for 52 hours in SPS or α-MEM. At 4, 16 and 52 hours, SPS and α-MEM were collected from the wells and (B) Ca^{2+} and PO_4^{3-} concentrations were measured by ICP-OES.

Fourier transformed infrared spectroscopy

Ceramic particles that remained in the tubes after removing solutions for ICP-OES analysis were transferred to new tubes and dried at room temperature for analysis using Fourier transformed infrared spectroscopy (FTIR, Perkin-Elmer Spectrum 1000).

Scanning electron microscopy

Samples for scanning electron microscopy (SEM) were fixed in 10% formalin (Sigma), dehydrated in an ethanol gradient series and dried using critical point dryer equipment (CPD 030, BAL-TEC). The samples were then gold-sputtered and imaged with SEM in secondary electron mode (XL30 ESEM-FEG, Philips). In the case of samples without cells, only the dehydration and subsequent steps were performed.

Cell culture and proliferation

MSC were previously characterized as multipotent and comply with the standard CD marker panel that defines MSC.[17] MSC were isolated from bone marrow aspirates (5–20 ml) obtained from donors with written informed consent. Aspirates were resuspended using 20 G needles, plated at a density of 5×10^5 cells per cm^2 and cultured in proliferation medium (PM), consisting of α-MEM (Gibco), 10% foetal bovine serum (Lonza), 2 mM L-glutamine (Gibco), 0.2 mM ascorbic acid (Sigma), 100 U ml^{-1} penicillin and 100 μg ml^{-1} streptomycin (Gibco) (Basic Medium, BM) supplemented with 1 ng ml^{-1} rhbFGF (AbDSerotec). MSC were expanded at an initial seeding density of 1000 cells per cm^2 in PM and medium was refreshed every 2 to 3 days. Cells were harvested at approximately 80% confluency for subculture. Cell culturing took place in a 5% CO_2 humid atmosphere at 37 °C. All experiments were performed in compliance with the relevant laws and institutional guidelines of the Medisch Spectrum Twente Medisch Ethische Toetsings Commissie.

MSC culture on ceramic scaffolds

HA and β-TCP were incubated in BM for 4 hours prior to cell seeding for optimal infiltration of medium into the ceramic pores and protein adsorption to the surface. Three particles of either HA or β-TCP were placed in one corner in squared wells of polystyrene plates. A cell suspension of 100 μl MSC in passage 2 or 3 in BM was pipetted on top of each particle set. To ensure maximum cell adhesion to the ceramic surface, plates were tilted to avoid cell dispersion throughout the well. Cells were allowed to attach for 4 hours after which 2 ml of osteogenic differentiation medium (OM; BM containing 10 nM dexamethasone (Sigma)) were slowly added to each sample. OM was refreshed every 2 days. MSC cultured in β-TCP or HA are referred to as MSC-TCP and MSC-HA respectively.

Table 1 Human primers' sequences

Name	Primer sequences
18S	5′-CGGCTACCACATCCAAGGAA-3′ 5′-GCTGGAATTACCGCGGCT-3′
OC	5′-GGCAGCGAGGTAGTGAAGAG-3′ 5′-GATGTGGTCAGCCAACTCGT-3′
BSP	5′-TGCCTTGAGCCTGCTTCC-3′ 5′-CAAAATTAAAGCAGTCTTCATTTTG-3′
OP	5′-CCAAGTAAGTCCAACGAAAG-3′ 5′-GGTGATGTCCTCGTCTGTA-3′
BMP-2 RGS2 GPRC5A BHLHE40	Commercially bought (SA Biosciences)

RNA isolation and gene expression analysis using quantitative qPCR

Total RNA was isolated from biological triplicates of MSC-TCP or MSC-HA after 12 hours, 2, 3, 5 and 7 days of culturing using a combination of the TRIzol (Invitrogen) method with the NucleoSpinRNA II isolation kit (Macherey-Nagel). Samples were rinsed in PBS and 1 ml of TRIzol reagent was added. After 1 freeze–thaw cycle, 200 μl chloroform was added per sample followed by centrifugation to achieve phase separation. The aqueous phase, containing the RNA, was collected, mixed with an equal volume of 75% ethanol and loaded onto the RNA binding column of the NucleoSpinRNA II isolation kit. Subsequent steps were in accordance with the manufacturer's protocol. RNA was collected in RNAse-free water. The quality and quantity of total RNA were analysed using gel electrophoresis and spectrophotometry.

First strand cDNA was synthesized using iScript (Bio-Rad) according to the manufacturer's protocol. One μl of undiluted cDNA was used for quantitative real time PCR performed on a Light Cycler PCR machine (Roche) using SYBR green I master mix (Invitrogen). For 18S amplification, cDNA was diluted 100×. The PCR amplifications were run under the following conditions: initial denaturation for 5 minutes at 95 °C, then cycled 45 times at 95 °C for 15 seconds, specific annealing temperature for 30 seconds and 72 °C for 30 seconds, followed by a melting curve. Primer sequences can be found in Table 1. PCR data were analysed using Light Cycler software version 3.5.3, using the fit point method by setting the noise band to the exponential phase of the reaction to exclude background fluorescence. Expression of all genes was normalised to 18S levels and fold inductions were calculated using the comparative ΔCT method.

cRNA synthesis and whole genome microarray analysis

Total RNA was isolated as described before, from biological triplicates of MSC-TCP or MSC-HA after 12 hours and 2 days of culturing. RNA concentration was determined by absorbance at 260 nm using the Nanodrop ND-1000 and quality and integrity were verified using the RNA 6000 Nano assay on the Agilent 2100 Bioanalyzer (Agilent Technologies). Next, 100 ng of total RNA was used for transcriptional profiling with Affymetrix 3′ IVT microarray analysis (Affymetrix, Santa Clara, CA, USA) using the Affymetrix 3′ IVT Express Kit (part nr. 901229) to generate Biotin-labeled antisense cRNA. cRNA quality was assessed using the Agilent 2100 Bioanalyzer. The labeled cRNA was used for hybridization to Affymetrix HT HG U133+ PM 16-Array Plate following the Affymetrix 3′ IVT Express manual. After an automated process of washing and staining by the GeneTitan machine (Affymetrix, Santa Clara, CA, USA) using the Affymetrix HWS Kit for GeneTitan (part nr. 901530), absolute values of expression were calculated from the scanned array using the Affymetrix Command Console v3 software.

Further analysis was performed using the RDN normalization toolbox.[18] After normalization, genes were ranked based on their fold change difference between β-TCP and HA materials, for each separate time point. Using the rank product test,[19] a combined list was created with genes that showed consistent high fold changes at both time points. The False Discovery Rate (FDR) was used to correct for multiple testing.

Statistical analysis

Statistical analysis is indicated in the respective figure legends. Error bars indicate standard deviation. For all figures the following applies: $*p < 0.05$; $**p < 0.01$; $***p < 0.001$.

Results

Ca^{2+} and PO_4^{3-} release profiles from β-TCP and HA

Fig. 1B depicts the results obtained on $[Ca^{2+}]$ and PO_4^{3-} concentration $[PO_4^{3-}]$ using ICP-OES. Immersion of β-TCP in SPS resulted in a continuous increase of both $[Ca^{2+}]$ and $[PO_4^{3-}]$, to a level of 8 and 19 ppm, respectively, after 52 hours. Neither Ca^{2+} nor PO_4^{3-} was detected in SPS after immersion of HA for the time points tested. Considering $[Ca^{2+}]$ measured upon immersion of ceramics in α-MEM, initially, this was 31.6 and 33.6 ppm for β-TCP and HA respectively. In both β-TCP and HA incubation solutions, the $[Ca^{2+}]$ increased to 32.5 to 34.1 ppm from 4 to 16 hours, respectively, and after that dropped to approximately 28 ppm in both cases. Regarding PO_4^{3-} dissolution, all values were close to 20 ppm at 4 and 16 hours. However the $[PO_4^{3-}]$ decreased between 16 and 52 hours to approximately 17 ppm in both HA and β-TCP incubation solutions. Blank measurements in α-MEM showed a decrease in $[PO_4^{3-}]$ from 16 to 52 hours.

Measurements in SPS demonstrate the higher solubility of β-TCP *versus* HA. The decreasing values of $[Ca^{2+}]$ and $[PO_4^{3-}]$ in α-MEM in time possibly reflect super saturation of Ca^{2+} and PO_4^{3-} in solution and consequent precipitation on both β-TCP and HA.

FTIR spectra of HA and TCP

$[Ca^{2+}]$ and $[PO_4^{3-}]$ measurements in SPS suggested a continuous dissolution of ions, at least in the case of β-TCP, and measurements in α-MEM suggested precipitation of CaP salts on both ceramics. Therefore we hypothesized that the chemical composition of the ceramics was changing in time due to dissolution/precipitation events.

Following a similar experimental setup depicted in Fig. 1A, but collecting the ceramics instead of the incubation solutions (Fig. S1A, ESI†), FTIR analysis was performed on bulk ceramics immersed for 52 hours in SPS and α-MEM and in addition, on a sample immersed in BM. No obvious differences in the FTIR spectra were observed between the conditions tested.

HA and β-TCP surface imaging

To assess whether signs of dissolution/precipitation events were visible on HA and β-TCP, we imaged the surfaces before (blank) and after immersion in SPS, α-MEM or BM for 2 days, the results of which are shown in Fig. 2.

In the blank images, it can be appreciated that the grains of HA surfaces are larger than those of β-TCP and that HA has fewer micropores, as was previously shown.[14] After 2 days of incubation in SPS, no considerable changes in surface morphology were observed in either ceramic. However, after immersion in α-MEM, surfaces of both HA and β-TCP were covered with crystals that grew perpendicular to the ceramic surface (Fig. 2, high magnification). Immersion in BM resulted in irregular precipitates of approximately 1 to 2 μm in size, heterogeneously distributed throughout the β-TCP surface, while no obvious surface change was detected in BM-immersed HA.

The surfaces of β-TCP and HA exhibited a new crystalline phase when immersed in α-MEM, but not when immersed in SPS or BM for 2 days.

MSC attachment and spreading at early time points

Next, we investigated MSC adhesion to the ceramic particles. We pre-wetted β-TCP and HA in BM for four hours and then seeded 600 000 MSC per 3 particles of either HA or β-TCP. After 4 hours, 2 ml of OM were added per sample and 4 hours and 1 day later, samples were imaged with SEM (Fig. 3).

After four hours, individual cells could be distinguished on HA but their adhesion to the surface seemed to be less strong than that of MSC spread on the β-TCP surface. After 1 day, similar images were obtained, showing that MSC were well spread on β-TCP (white arrows in Fig. 3) whereas in HA patches of poorly adhered MSC were seen.

MSC-TCP *vs.* MSC-HA osteogenic profile

We knew, from previous work, that after 7 days of culture, MSC-TCP express higher levels of OP, OC and BSP than MSC-HA.[14] Since our most recent work correlates Ca^{2+} with expression of the aforementioned genes and with that of BMP-2,[15] we analysed expression of all four genes in MSC-TCP and MSC-HA, to investigate up to which extent the expression of osteogenic markers correlates between β-TCP and high content Ca^{2+} medium, and HA and low content Ca^{2+} medium, respectively. Results from 2 donors (Fig. 4) show that expression of OC and OP was significantly higher in MSC-TCP than in MSC-HA. Although differences between MSC-TCP and MSC-HA were not statistically significant for any donor in the case of BMP-2 or BSP, MSC-TCP exhibited a consistent higher expression of BMP-2 than MSC-HA.

Next, we analysed the expression of the same genes at 12 hours, 2, 3, 5 and 7 days to see whether the gene expression differences between MSC-TCP and MSC-HA could be detected earlier than day 7. As shown in Fig. 5, differential gene expression between the two conditions was only visible, in general, after day 5. At this time point, however, MSC-TCP expressed 3 times more BMP-2 than MSC-HA, in line with what was observed before (Fig. 4). At day 7, expression of OC, OP and BSP was always higher in MSC-TCP. Most profound was the expression of OP, which was 40 times higher in MSC-TCP than in MSC-HA.

These experiments demonstrate that β-TCP promotes upregulation of OC, OP, BSP and BMP-2 expression in MSC, compared to HA. Before day 5, however, there was no statistical significant differential gene expression between MSC-TCP and MSC-HA for the markers analysed.

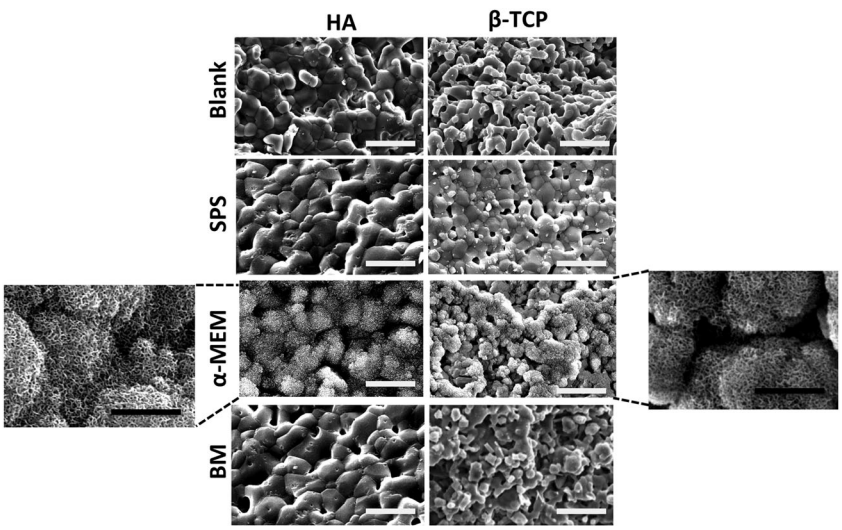

Fig. 2 HA and β-TCP surfaces after immersion in different solutions. HA and β-TCP surfaces were imaged with SEM before (blank) and after incubation in SPS, α-MEM and BM for 2 days. A new crystalline phase can be observed in HA and β-TCP after immersion in α-MEM. BM and SPS did not significantly affect HA and β-TCP surfaces. White and black scale bars represent, respectively, 5 and 2 μm.

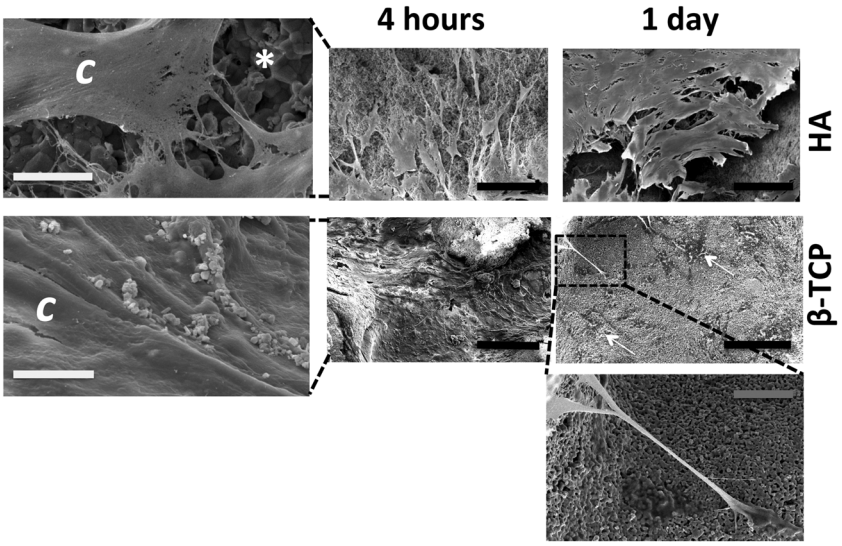

Fig. 3 MSC attached and spread better on β-TCP than on HA. MSC were seeded on HA or β-TCP and cultured for 4 hours and 1 day. Cells attached to the ceramic surface were visualized with SEM. In β-TCP, MSC were well attached and spread on the ceramic whereas in HA they loosely touch the surface at both time points. Far left images show details of cells (c) attached and spreading on the ceramic surfaces (*) after 4 hours. White arrows point towards MSC spread on the β-TCP surface and the inset image provides details of filopodia-like structure. White, grey and black scale bars represent, respectively, 10, 20 and 100 μm.

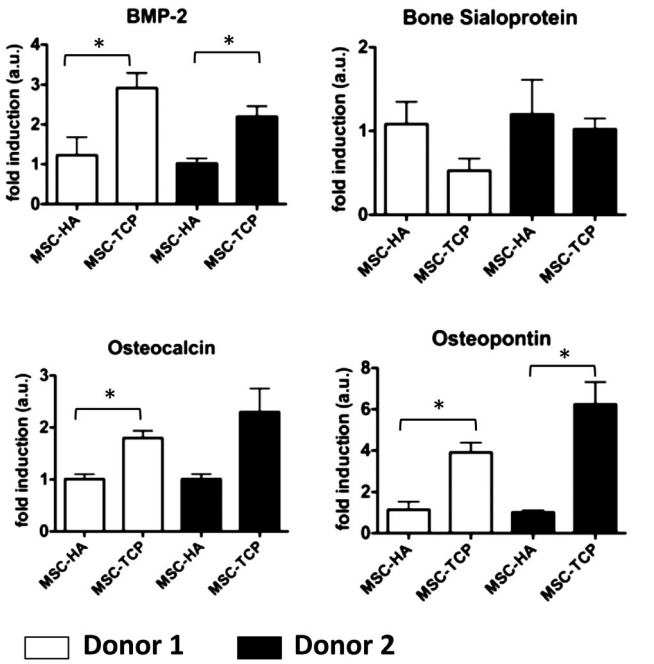

Fig. 4 Gene expression profile of MSC-TCP *vs.* MSC-HA is consistent among different donors. MSC from donors 1 (white bars) and 2 (black bars) were cultured on HA and β-TCP for 7 days in OM. At that time point, expression of BMP-2, osteopontin, osteocalcin and bone sialoprotein (BSP) was analyzed. MSC-TCP showed higher expression of those genes in all donors, except for BSP. Statistical analysis was done using a student *t*-test for the individual donors ($p < 0.05$ and $n = 3$).

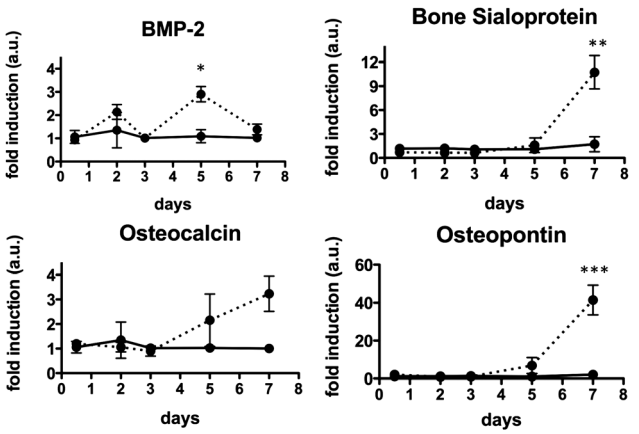

Fig. 5 MSC-TCP exhibit stronger osteogenic profile than MSC-HA in time. MSC from donor 3 were cultured on HA and β-TCP for 12 hours, 2, 3, 5 and 7 days in OM. At each time point, expression of BMP-2, osteopontin, osteocalcin and bone sialoprotein was analyzed. Statistical significant differences were observed at the late time points between MSC-TCP (. . .) and MSC-HA (—). Statistical analysis was done with two-way Analysis of Variance (ANOVA) and Bonferroni post-tests ($p < 0.05$ and $n = 3$).

MSC-TCP *vs.* MSC-HA whole genome microarray

To further correlate extracellular signals provided by the ceramics with specific molecular and cellular responses at early stages of culturing, we performed a whole genome microarray. We decided to look for high fold changes in gene expression, at both 12 hours and 2 days, between MSC-TCP and MSC-HA, in order to find those genes that were early, strongly and consistently affected by β-TCP over HA. In Table 2, we report 70 genes that have a False Discovery Rate (FDR) of ≤ 0.10, as determined by the Rank Product test, that shows the largest difference in expression between β-TCP and HA, at both time points. The genes here shown will be later discussed in terms of relevant signaling pathways and biological functions. Also to provide insight into biological functions regulated by β-TCP, analysis with Gene Ontology enrichment was performed, based on 145 probe sets having a FDR < 0.2. Enriched biological process

Table 2 Genes consistently upregulated by β-TCP after 12 hours and 2 days

Gene symbol	Gene description	R_{FC1}	R_{FC2}	FDR
BHLHE40	Basic helix-loop-helix family, member e40	1	24	0.0020
GPRC5A	G protein-coupled receptor, family C, group 5, member A	5	14	0.0020
RGS2	Regulator of G-protein signaling 2, 24 kDa	36	2	0.0017
DDIT3///NR1H3	DNA-damage-inducible transcript 3///nuclear receptor subfamily 1, group H, member 3	120	5	0.0178
HES1	Hairy and enhancer of split 1 (Drosophila)	6	165	0.0280
GDF15///LOC100292463	Growth differentiation factor 15///similar to growth differentiation factor 15	2	534	0.0252
SLC2A3	Solute carrier family 2 (facilitated glucose transporter), member 3	137	9	0.0240
AMD1	Adenosylmethionine decarboxylase 1	4	488	0.0371
CTGF	Connective tissue growth factor	3	719	0.0368
ADM	Adrenomedullin	22	99	0.0337
AREG	Amphiregulin	2365	1	0.0335
SLC16A6	Solute carrier family 16, member 6 (monocarboxylic acid transporter 7)	77	32	0.0326
ITPR1	Inositol 1,4,5-triphosphate receptor, type 1	371	11	0.0495
GADD45B	Growth arrest and DNA-damage-inducible, beta	32	136	0.0496
NEAT1	Nuclear paraspeckle assembly transcript 1 (non-protein coding)	45	108	0.0517
RAB20	RAB20, member RAS oncogene family	19	273	0.0516
ERO1L	ERO1-like (*S. cerevisiae*)	275	21	0.0546
HNRNPAB	Heterogeneous nuclear ribonucleoprotein A/B	7	830	0.0519
GADD45B	Growth arrest and DNA-damage-inducible, beta	50	122	0.0516
ATF3	Activating transcription factor 3	246	26	0.0515
PPP1R3C	Protein phosphatase 1, regulatory (inhibitor) subunit 3C	41	158	0.0497
SIK1	Salt-inducible kinase 1	14	464	0.0475
AMIGO2	Adhesion molecule with Ig-like domain 2	8	878	0.0504
FAM98A	Family with sequence similarity 98, member A	16	476	0.0539
C10orf10	Chromosome 10 open reading frame 10	1912	4	0.0520
C13orf33	Chromosome 13 open reading frame 33	312	25	0.0513
CDCA2	Cell division cycle associated 2	78	113	0.0566
PTGS2	Prostaglandin-endoperoxide synthase 2 (prostaglandin G/H synthase and cyclooxygenase)	191	49	0.0564
VEGFA	Vascular endothelial growth factor A	150	64	0.0562
KYNU	Kynureninase (L-kynurenine hydrolase)	60	162	0.0550
GPATCH4	G patch domain containing 4	27	376	0.0556
RYBP	RING1 and YY1 binding protein	47	243	0.0608
VEGFA	Vascular endothelial growth factor A	126	92	0.0599
DUSP10	Dual specificity phosphatase 10	142	83	0.0594
SLC2A14///SLC2A3	Solute carrier family 2 (facilitated glucose transporter), member 14///solute carrier family 2 (facilitated glucose transporter), member 3	2008	6	0.0591
GADD45B	Growth arrest and DNA-damage-inducible, beta	99	127	0.0598
NOP56	NOP56 ribonucleoprotein homolog (yeast)	31	457	0.0667
IRS2	Insulin receptor substrate 2	90	169	0.0701
UHRF1	Ubiquitin-like with PHD and ring finger domains 1	55	314	0.0779
IER3	Immediate early response 3	108	160	0.0760
PITPNC1	Phosphatidylinositol transfer protein, cytoplasmic 1	80	218	0.0749
CXCR4	Chemokine (C-X-C motif) receptor 4	1499	13	0.0824
RRAGD	Ras-related GTP binding D	281	71	0.0810
C10orf10	Chromosome 10 open reading frame 10	268	76	0.0810
RORA	RAR-related orphan receptor A	51	402	0.0800
UGP2	UDP-glucose pyrophosphorylase 2	318	67	0.0818
NEAT1	Nuclear paraspeckle assembly transcript 1 (non-protein coding)	194	114	0.0837
CLEC2B	C-type lectin domain family 2, member B	2885	8	0.0863
EGLN3	egl nine homolog 3 (*C. elegans*)	118	220	0.0939
TFRC	Transferrin receptor (p90, CD71)	12	2167	0.0924
SLC2A3	Solute carrier family 2 (facilitated glucose transporter), member 3	219	119	0.0908
ABCE1	ATP-binding cassette, sub-family E (OABP), member 1	40	655	0.0897
RIPK4	Receptor-interacting serine-threonine kinase 4	135	198	0.0900
RORA	RAR-related orphan receptor A	1578	17	0.0888
DSEL	Dermatan sulfate epimerase-like	20	1354	0.0881
NAP1L3	Nucleosome assembly protein 1-like 3	76	372	0.0888
SLC26A2	Solute carrier family 26 (sulfate transporter), member 2	15	2008	0.0932
ELL2	Elongation factor, RNA polymerase II, 2	996	31	0.0934
IL8	Interleukin 8	10313	3	0.0921
STC2	Stanniocalcin 2	98	322	0.0927
LOC729222///PPFIBP1	Similar to PTPRF interacting protein binding protein 1///PTPRF interacting protein, binding protein 1 (liprin beta 1)	1026	33	0.0983
GPATCH4	G patch domain containing 4	46	738	0.0972
GALNTL2	UDP-*N*-acetyl-alpha-D-galactosamine:polypeptide *N*-acetylgalactosaminyltransferase-like 2	800	44	0.0997

Table 2 (*continued*)

Gene symbol	Gene description	R_{FC1}	R_{FC2}	FDR
IGFBP1	Insulin-like growth factor binding protein 1	186	190	0.0987
NOP16	NOP 16 nuclear protein homolog (yeast)	44	841	0.1011
AKAP12	A kinase (PRKA) anchor protein 12	58	650	0.1015

R_{FC1}/R_{FC2}: position in the rank of genes according to fold change on day 1 (FC1) or day 2 (FC2) (the larger the fold change, the lower the rank); FDR: false discovery rate.

Table 3 Selected enriched gene ontology clusters (following DAVID[20]) from the top 15 displayed in ST1, based on the set of consistently induced genes affected by β-TCP after 12 hours and 2 days (FDR < 0.2). Right column displays the symbol of genes corresponding to the respective biological process terms

AC	Biological process terms	FDR	Gene symbol
2 Enrichment Score: 2.275123253708776			
	GO:0001503 ~ ossification	0.0394	SLC26A2; CNKSR1; IGFBP3; CNGF; STC1; STC1;
	GO:0060348 ~ bone development	0.0485	SCL26A2; BMP2; MMP13; PTGS2; BMP2
	GO:0001501 ~ skeletal system development	0.1911	STC1; BMP2; MMP13; PTGS2; BMP2; SLC26A2; CNGF; CTNNB1; IGFBP3; PTGS2; STC1; SLC26A2; ZFAND5
13 Enrichment Score: 1.2705300327366442			
	GO:0001569 ~ patterning of blood vessels	0.0742	VEGFA; CXCR4; CTNNB1; CXCR4; VEGFA
	GO:0048754 ~ branching morphogenesis of a tube	0.1593	VEGFA; CXCR4; CTNNB1; BMP2; CXCR4; VEGFA; BMP2
	GO:0001763 ~ morphogenesis of a branching structure	0.1857	
	GO:0035239 ~ tube morphogenesis	0.1958	
14 Enrichment Score: 1.2532056572273087			
	GO:0055066 ~ di-, tri-valent inorganic cation homeostasis	0.1456	ITPR1; TFRC; CXCR4; SOD2; STC1; ITPR1; ITPR1; CXCR4; TFRC; ADM; STC1; MCHR1; HERPUD1
	GO:0055080 ~ cation homeostasis	0.2352	
	GO:0030005 ~ cellular di-, tri-valent inorganic cation homeostasis	0.2217	ITPR1; TFRC; TFRC; CXCR4; STC1; STC1; ADM; ITPR1; MCHR1; ITPR1; CXCR4; HERPUD1
	GO:0006874 ~ cellular calcium ion homeostasis	0.2620	ITPR1; CXCR4; STC1; STC1; ADM; ITPR1; MCHR1; ITPR1; CXCR4; HERPUD1
	GO:0006873 ~ cellular ion homeostasis	0.3333	ITPR1; TFRC; CXCR4; GRIN2A; SOD2; STC1; ITPR1; ITPR1; CXCR4; TFRC; STC1; ADM; MCHR1; HERPUD1
	GO:0055074 ~ calcium ion homeostasis	0.2761	IPTR1; CXCR4; STC1; STC1; ADM; ITPR1; MCHR1; ITPR1; CXCR4; HERPUD1
	GO:0055082 ~ cellular chemical homeostasis	0.3534	ITPR1; TFRC; CXCR4; GRIN2A; SOD2; STC1; ITPR1; ITPR1; CXCR4; TFRC; STC1; ADM; MCHR1; HERPUD1
	GO:0030003 ~ cellular cation homeostasis	0.3257	ITPR1; TFRC; TFRC; CXCR4; STC1; STC1; ADM; ITPR1; MCHR1; ITPR1; CXCR4; HERPUD1
	GO:0006875 ~ cellular metal ion homeostasis	0.3152	ITPR1; CXCR4; STC1; STC1; ADM; ITPR1; MCHR1; ITPR1; CXCR4; HERPUD1
	GO:0019725 ~ cellular homeostasis	0.4416	ITPR1; TFRC; CXCR4; GRIN2A; SOD2; STC1; ITPR1; ITPR1; DDIT3; CXCR4; TFRC; STC1; ADM; MCHR1; HERPUD1
	GO:0055065 ~ metal ion homeostasis	0.3604	ITPR1; CXCR4; STC1; STC1; ADM; ITPR1; MCHR1; ITPR1; CXCR4; HERPUD1
	GO:0050801 ~ ion homeostasis	0.4697	ITPR1; TFRC; CXCR4; GRIN2A; SOD2; STC1; ITPR1; DDIT3; CXCR4; TFRC; STC1; ADM; MCHR1; HERPUD1

AC: annotation cluster number; FDR: false discovery rate; N.B.: the multiple testing correction is too conservative, as it does not take into account the similarity between many GO terms.

terms were clustered on functional similarity to enhance their interpretability, using the method made available by DAVID.[20] In Table 3, three clusters from the top 15 are presented, whereas all enriched clusters are shown in Table S1 (ESI†).

Expression of genes in the top 3 of Table 2 (RGS2, GPCR5A and BHLH40) was further confirmed by qPCR analysis. RGS2 and GPCR5A were upregulated in MSC-TCP compared to MSC-HA (Fig. 6) after 2 days, but not after 12 hours. For BHLHE40, results were consistent with the microarray, but not statistically significant.

Discussion

In this manuscript, we analysed the expression of osteogenic markers in MSC grown on β-TCP and HA (Fig. 4 and 5), and using microarray analysis, we discovered novel genes whose expression is strongly evoked by β-TCP at early time points of culture (Table 2 and Fig. 6). Furthermore, we tried to correlate the solubility of β-TCP and HA (Fig. 1, 2 and Fig. S1, ESI†) with our biological findings, as based on our previous work, and we hypothesized that this might be a key physico-chemical parameter in mediating the bioactivity of these ceramics.

We have shown in the past that MSC exhibit an osteogenic phenotype in culture medium containing high [Ca^{2+}] (CaM). BMP-2 expression is induced within 6 hours after exposing MSC to CaM and, at later time points, OC, OP and BSP are induced as well.[15] In this manuscript, analysis of osteogenic marker genes also revealed higher expression of OC, OP, and BSP in MSC-TCP than in MSC-HA, consistent in all donors except for BSP. Furthermore, BMP-2 was also upregulated by MSC-TCP

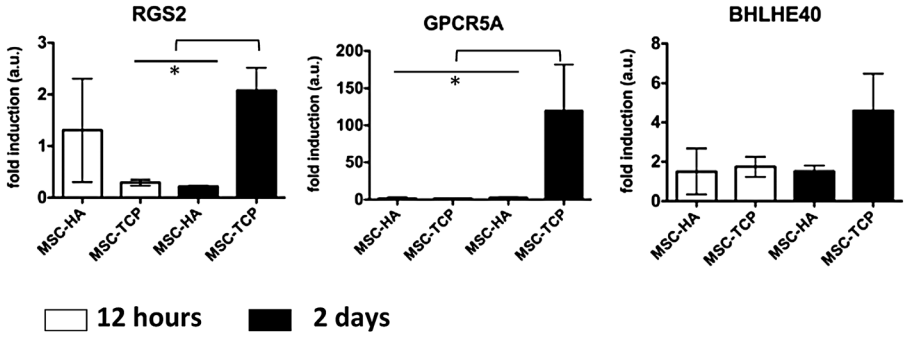

Fig. 6 Genes differentially regulated between MSC-TCP and MSC-HA analyzed by PCR. DNA microarray analysis showed that the top scored genes regulated by β-TCP were RGS2, GPCR5A and BHLHE40 (Table 2). Fold induction of RGS2, GPCR5A and BHLHE40 measured by PCR shows that after 12 hours (white bars) there were no statistically significant differences between MSC-TCP and MSC-HA, whereas after 2 days there are in the case of RGS2 and GPCR5A. Statistical analysis was performed with one-way ANOVA and Tukey's multiple comparison post-test ($p < 0.05$ and $n = 3$).

compared to MSC-HA (day 5) and earlier than the other genes. Although with a different timing, this resemblance in the osteogenic response between MSC-TCP and MSC cultured in CaM further suggests that the high solubility of β-TCP provides an enriched Ca^{2+} environment to MSC, which could be an important driving factor for the observed osteogenic differentiation.

This is also supported by an earlier reported effect of Ca^{2+} on osteogenic differentiation of human periosteal derived stem cells (PD-MSC). PD-MSC cultured in the presence of Ca^{2+}, exhibited expression of BMP-2, OC, OP and BSP, in a dose dependent fashion.[21,22] Furthermore, PD-MSC seeded onto Collagraft™ and implanted subcutaneously in nude mice induced bone formation, whereas when Collagraft™ was decalcified prior to cell seeding (*i.e.* removal of Ca^{2+} and PO_4^{3-}), bone formation was abrogated,[23] suggesting the relevance of the construct's mineral composition.

The high solubility of β-TCP was demonstrated in SPS (Fig. 1). SPS is an *in vitro* solution resembling pH and ionic strength of human blood plasma (obtained by dissolution of NaCl salt), however it is, in contrast to blood plasma, not saturated towards calcium phosphates (dicalcium phosphate dihydrate, octacalcium phosphate, HA). Upon immersion of any calcium-phosphate ceramic, release of calcium and phosphate ions will occur, the extent of which depends on the solubility of the calcium-phosphate phase as well as other physical properties of the ceramic. Since β-TCP is much more soluble than HA, continuous release of both calcium and ions was observed during 56 hour experiment. Release of ions from HA was too low to be determined within 56 hours.

α-MEM, the basic constituent of the cell culture medium used in these experiments, contains both calcium and phosphate ions, thus its mineral composition differs from that of SPS. In α-MEM, the possibility of obtaining supersaturation of calcium and phosphate ions (from the medium itself and/or as a result of ceramic degradation) in the vicinity of the ceramic, followed by precipitation of new calcium-phosphate crystals on the ceramic surface (as shown in Fig. 2), is therefore much larger than in SPS. This process of dissolution/reprecipitation is continuous, and will eventually occur faster in the more soluble ceramic. However, considering that release experiments were limited to 56 hours in the present study, no obvious differences between the two ceramics immersed in α-MEM could be measured.

When immersed in BM, however, HA and β-TCP surfaces were similar to those observed in the blank and SPS-immersed ceramics (Fig. 2). The presence of proteins in BM may have impeded the development of a new crystalline phase, as proteins are known to affect the original nucleation or crystal growth rate observed in CaP ceramics.[24,25] Though the presence of irregular precipitates was detected in BM, these were possibly due to precipitation of NaCl. Furthermore FTIR data did not reveal any significant differences in the chemical composition of samples analysed at day 2, perhaps because surface changes were of too low magnitude to be detected in the midst of the bulk.

Although we did not detect differences in the surface dynamics of HA and β-TCP when immersed in BM (FTIR and SEM), microarray data analysis showed evidence of ongoing inorganic cation homeostasis and in particular Ca^{2+} homeostasis upregulation by β-TCP compared to HA (Table 3), already 12 hours and 2 days after cell seeding. This could indicate that $[Ca^{2+}]$ in the vicinity of β-TCP is sufficient to affect cellular behavior without significantly altering the crystalline phase of the surface (Fig. 2) and that perhaps $[Ca^{2+}]$ increases in time, later inducing expression of OP, OC, BSP and BMP-2 (days 5 and 7). In fact, cluster 2 of the GO enrichment showed that ossification, skeletal development and bone development were upregulated functions in MSC-TCP compared to MSC-HA, suggesting that the microarray data are in line with later PCR observations on osteogenic markers expression. Thus, our biological data suggest that MSC-TCP sensed higher $[Ca^{2+}]$ compared with MSC-HA.

Regarding the top genes in Table 2, it is interesting to note that GPCR5A and the regulator of G-protein signaling (RGS2) are related with G-protein coupled receptor (GPCR) signaling.[26] Expression of these genes was further confirmed by PCR, showing that RGS2 and GPCR5A were expressed, respectively, 10 and 100 times more in MSC-TCP than in MSC-HA at day 2. At 12 hours differential expression was not confirmed by PCR. In particular, RGS2 has been linked with osteogenic differentiation and osteoblasts proliferation[27–29] and its expression can be regulated by cAMP.[30] Expression of GPCR5A, also known as

retinoic acid inducible gene 1 (RAIG1), has been linked with differentiation and maintenance of homeostasis in epithelial cells and maturation of lung and kidney during embryonic development.[31] Furthermore GPCR5A expression has been associated with cancer development.[32] Over expression of this gene also led to a decrease in cAMP accumulation and Gsα down regulation.[33]

Genes coding for members of the Protein Kinase A (PKA) signaling cascade, regulated by cAMP cytosolic accumulation, which is downstream of GPCR signaling, also appear in Table 2. For instance, A kinase anchor protein 12 (AKAP12) binds to PKA and drives its subunits within the cell. Furthermore, both ATF3 and HES1 transcription is regulated by cAMP response element binding (CREB),[34,35] supporting a strong upregulation of the PKA signalling pathway by β-TCP compared to HA. In addition, SIK1 is a PKA target protein[36] and GDF15, CTGF and amphiregulin expression are PKA dependent as well.[37–39] Future experiments will be aimed at looking in more detail at the involvement of PKA signaling in MSC-TCP induced gene expression and at identifying the molecules responsible for the induction.

Furthermore other genes regulated by β-TCP have been previously linked to osteogenesis, such as GDF15[40] and BHLHE40[41,42] and interestingly with angiogenesis, VEGFA[43] and IL-8,[44] further suggesting that β-TCP might not only have a pro-osteogenic effect but also a pro-angiogenic one. Indeed cluster 13 shows enrichment of terms related with blood vessel formation.

Although we suggest that Ca^{2+} dissolution plays a role in osteogenesis of MSC cultured in β-TCP, we do not exclude the effect of other physico-chemical parameters. We have also shown that MSC attachment and spreading are different between HA and β-TCP, as suggested by SEM analysis, which was not further explored here. Differences in cell attachment could be due to different microstructure or charge of these materials that lead to differential protein adsorption and consequent differential focal adhesion assembly.

Conclusion

We confirmed higher solubility of β-TCP in SPS when compared to HA, although a clear link between Ca^{2+} dissolution from β-TCP and osteogenesis of MSC could not be established. However, microarray analysis detected upregulation of Ca^{2+} homeostasis in MSC-TCP after 12 and 48 hours of culturing as compared to MSC-HA, and furthermore PCR analysis showed that β-TCP significantly increased expression of genes in MSC that are characteristics of high [Ca^{2+}] content medium, such as BMP-2, OP, OC and BSP. Furthermore, microarray analysis showed that GPCR signaling and PKA pathways are strongly upregulated by β-TCP over HA.

Acknowledgements

The authors gratefully acknowledge the technical support from the Katholieke Universiteit Leuven and the financial support from the TeRM Smart Mix Program of the Netherlands Ministry of Economic Affairs and The Netherlands Ministry of Education, Culture and Science, BMM (ZT, AB) and STW Vernieuwingsimpuls Veni (PH).

References

1 T. A. St John, A. R. Vaccaro, A. P. Sah, M. Schaefer, S. C. Berta, T. Albert and A. Hilibrand, Physical and monetary costs associated with autogenous bone graft harvesting, *Am. J. Orthop.*, 2003, **32**(1), 18–23.
2 C. J. Damien and J. R. Parsons, Bone graft and bone graft substitutes: a review of current technology and applications, *J. Appl. Biomater.*, 1991, **2**(3), 187–208.
3 J. F. Brandoff, J. S. Silber and A. R. Vaccaro, Contemporary alternatives to synthetic bone grafts for spine surgery, *Am. J. Orthop.*, 2008, **37**(8), 410–414.
4 P. V. Giannoudis, H. Dinopoulos and E. Tsiridis, Bone substitutes: an update, *Injury*, 2005, **36**(suppl. 3), S20–S27.
5 G. M. Calori, E. Mazza, M. Colombo and C. Ripamonti, The use of bone-graft substitutes in large bone defects: any specific needs?, *Injury*, 2011, **42**(suppl. 2), S56–S63.
6 J. Van der Stok, E. M. M. Van Lieshout, Y. El-Massoudi, G. H. Van Kralingen and P. Patka, Bone substitutes in the Netherlands – a systematic literature review, *Acta Biomater.*, 2011, **7**(2), 739–750.
7 A. M. C. Barradas, H. Yuan, C. A. van Blitterswijk and P. Habibovic, Osteoinductive biomaterials: current knowledge of properties, experimental models and biological mechanisms, *Eur. Cell Mater.*, 2011, **21**, 407–429.
8 G. Daculsi, O. Laboux, O. Malard and P. Weiss, Current state of the art of biphasic calcium phosphate bioceramics, *J. Mater. Sci. Mater. Med.*, 2003, **14**(3), 195–200.
9 A. Hoppe, N. S. Guldal and A. R. Boccaccini, A review of the biological response to ionic dissolution products from bioactive glasses and glass-ceramics, *Biomaterials.*, 2011, **32**(11), 2757–2774.
10 A. Matsushima, N. Kotobuki, M. Tadokoro, K. Kawate, H. Yajima, Y. Takakura and H. Ohgushi, *In vivo* Osteogenic Capability of Human Mesenchymal Cells Cultured on Hydroxyapatite and on β-Tricalcium Phosphate, *Artif. Organs*, 2009, **33**(6), 474–481.
11 Y. Tan, G. Wang, H. Fan, X. Wang, J. Lu and X. Zhang, Expression of core binding factor 1 and osteoblastic markers in C2C12 cells induced by calcium phosphate ceramics *in vitro*, *J. Biomed. Mater. Res., Part A*, 2007, **82**(1), 152–159.
12 A. Bernhardt, A. Lode, F. Peters and M. Gelinsky, Novel ceramic bone replacement material Osbone (R) in a comparative *in vitro* study with osteoblasts, *Clin. Oral Implants Res.*, 2011, **22**(6), 651–657.
13 C. Wang, Y. Duan, B. Markovic, J. Barbara, C. R. Howlett, X. Zhang and H. Zreiqat, Phenotypic expression of bone-related genes in osteoblasts grown on calcium phosphate ceramics with different phase compositions, *Biomaterials*, 2004, **25**(13), 2507–2514.
14 H. Yuan, H. Fernandes, P. Habibovic, J. de Boer, A. M. Barradas, A. de Ruiter, W. R. Walsh, C. A. van Blitterswijk

and J. D. de Bruijn, Osteoinductive ceramics as a synthetic alternative to autologous bone grafting, *Proc. Natl. Acad. Sci. U. S. A.*, 2010, **107**(31), 13614–13619.

15 A. M. C. Barradas, H. A. M. Fernandes, N. Groen, Y. C. Chai, J. Schrooten, J. van de Peppel, J. P. T. M. van Leeuwen, C. A. van Blitterswijk and J. de Boer, A calcium-induced signaling cascade leading to osteogenic differentiation of human bone marrow-derived mesenchymal stromal cells, *Biomaterials*, 2012, **33**(11), 3205–3215.

16 S. Li, J. R. de Wijn, J. Li, P. Layrolle and K. de Groot, Macroporous Biphasic Calcium Phosphate Scaffold with High Permeability/Porosity Ratio, *Tissue Eng.*, 2003, **9**(3), 535–548.

17 H. Alves, U. Munoz-Najar, J. De Wit, A. J. S. Renard, J. H. J. Hoeijmakers, J. M. Sedivy, C. Van Blitterswijk and J. De Boer, A link between the accumulation of DNA damage and loss of multi-potency of human mesenchymal stromal cells, *J. Cell. Mol. Med.*, 2010, **14**(12), 2729–2738.

18 M. Hulsman, A. Mentink, E. P. van Someren, K. J. Dechering, J. de Boer and M. J. T. Reinders, Delineation of amplification, hybridization and location effects in microarray data yields better-quality normalization, *BMC Bioinf.*, 2010, **11**, 156.

19 V. G. Tusher, R. Tibshirani and G. Chu, Significance analysis of microarrays applied to the ionizing radiation response, *Proc. Natl. Acad. Sci. U. S. A.*, 2001, **98**(9), 5116–5121.

20 D. W. Huang, B. T. Sherman, Q. Tan, J. Kir, D. Liu, D. Bryant, Y. Guo, R. Stephens, M. W. Baseler, H. C. Lane and R. A. Lempicki, DAVID Bioinformatics Resources: expanded annotation database and novel algorithms to better extract biology from large gene lists, *Nucleic Acids Res.*, 2007, **35**(suppl. 2), W169–W175.

21 Y. C. Chai, S. J. Roberts, J. Schrooten and F. P. Luyten, Probing the Osteoinductive Effect of Calcium Phosphate by Using an *In Vitro* Biomimetic Model, *Tissue Eng., Part A*, 2010, **17**(7–8), 1083–1097.

22 Y. C. Chai, S. J. Roberts, E. Desmet, G. Kerckhofs, N. van Gastel, L. Geris, G. Carmeliet, J. Schrooten and F. P. Luyten, Mechanisms of ectopic bone formation by human osteoprogenitor cells on CaP biomaterial carriers, *Biomaterials*, 2012, **33**(11), 3127–3142.

23 J. Eyckmans, S. J. Roberts, J. Schrooten and F. P. Luyten, A clinically relevant model of osteoinduction: a process requiring calcium phosphate and BMP/Wnt signaling, *J. Cell. Mol. Med.*, 2009, **14**(6B), 1845–1856.

24 C. Combes and C. Rey, Adsorption of proteins and calcium phosphate materials bioactivity, *Biomaterials*, 2002, **23**(13), 2817–2823.

25 S. Mann, Molecular recognition in biomineralization, *Nature*, 1988, **332**(6160), 119–124.

26 A. A. Roy, A. Baragli, L. S. Bernstein, J. R. Hepler, T. E. Hébert and P. Chidiac, RGS2 interacts with Gs and adenylyl cyclase in living cells, *Cell. Signalling*, 2006, **18**(3), 336–348.

27 A. Tsingotjidou, J. M. Nervina, L. Pham, O. Bezouglaia and S. Tetradis, Parathyroid hormone induces RGS-2 expression by a cyclic adenosine 3′,5′-monophosphate-mediated pathway in primary neonatal murine osteoblasts, *Bone*, 2002, **30**(5), 677–684.

28 M. Homme, C. P. Schmitt, R. Himmele, G. F. Hoffmann, O. Mehls and F. Schaefer, Vitamin D and Dexamethasone Inversely Regulate Parathyroid Hormone-Induced Regulator of G Protein Signaling-2 Expression in Osteoblast-Like Cells, *Endocrinology*, 2003, **144**(6), 2496–2504.

29 N. M. Teplyuk, M. Galindo, V. I. Teplyuk, J. Pratap, D. W. Young, D. Lapointe, A. Javed, J. L. Stein, J. B. Lian, G. S. Stein and A. J. van Wijnen, Runx2 Regulates G Protein-coupled Signaling Pathways to Control Growth of Osteoblast Progenitors, *J. Biol. Chem.*, 2008, **283**(41), 27585–27597.

30 Z. Xie, D. Liu, S. Liu, L. Calderon, G. Zhao, J. Turk and Z. Guo, Identification of a cAMP-response Element in the Regulator of G-protein Signaling-2 (RGS2) Promoter as a Key *Cis*-regulatory Element for RGS2 Transcriptional Regulation by Angiotensin II in Cultured Vascular Smooth Muscles, *J. Biol. Chem.*, 2011, **286**(52), 44646–44658.

31 Y. Cheng and R. Lotan, Molecular Cloning and Characterization of a Novel Retinoic Acid-inducible Gene That Encodes a Putative G Protein-coupled Receptor, *J. Biol. Chem.*, 1998, **273**(52), 35008–35015.

32 C. H. Chen, M. S. Benjamin, X. D. Sun, K. B. Otto, P. Guo, X. Y. Dong, Y. D. Bao, Z. M. Zhou, X. H. Cheng, J. W. Simons and J. T. Dong, KLF5 promotes cell proliferation and tumorigenesis through gene regulation in the TSU-Pr1 human bladder cancer cell line, *Int. J. Cancer*, 2006, **118**(6), 1346–1355.

33 M. Hirano, L. Zang, T. Oka, Y. Ito, Y. Shimada, Y. Nishimura and T. Tanaka, Novel reciprocal regulation of cAMP signaling and apoptosis by orphan G-protein-coupled receptor GPRC5A gene expression, *Biochem. Biophys. Res. Commun.*, 2006, **351**(1), 185–191.

34 H. Watanabe, M. J. Smith, E. Heilig, V. Beglopoulos, R. J. Kelleher and J. Shen, Indirect Regulation of Presenilins in CREB-mediated Transcription, *J. Biol. Chem.*, 2009, **284**(20), 13705–13713.

35 S. I. Mayer, V. Dexheimer, E. Nishida, S. Kitajima and G. Thiel, Expression of the Transcriptional Repressor ATF3 in Gonadotrophs Is Regulated by Egr-1, CREB, and ATF2 after Gonadotropin-Releasing Hormone Receptor Stimulation, *Endocrinology*, 2008, **149**(12), 6311–6325.

36 R. Berdeaux, N. Goebel, L. Banaszynski, H. Takemori, T. Wandless, G. D. Shelton and M. Montminy, SIK1 is a class II HDAC kinase that promotes survival of skeletal myocytes, *Nat. Med.*, 2007, **13**(5), 597–603.

37 T. Ichikawa, K. Horie-Inoue, K. Ikeda, B. Blumberg and S. Inoue, Vitamin K2 induces phosphorylation of protein kinase A and expression of novel target genes in osteoblastic cells, *J. Mol. Endocrinol.*, 2007, **39**(4), 239–247.

38 Y.-s. Guo, W.-j. Yuan, A.-p. Zhang, Y.-h. Ding and Y.-x. Wang, Parathyroid hormone-mitogen-activated protein kinase axis exerts fibrogenic effect of connective tissue growth factor on human renal proximal tubular cells, *Chin. Med. J.*, 2010, **123**(24), 3671–3676.

39 B. Du, N. K. Altorki, L. Kopelovich, K. Subbaramaiah and A. J. Dannenberg, Tobacco Smoke Stimulates the Transcription of Amphiregulin in Human Oral Epithelial Cells: Evidence of a Cyclic AMP-Responsive Element Binding Protein-Dependent Mechanism, *Cancer Res.*, 2005, **65**(13), 5982–5988.

40 P. Vanhara, E. Lincová, A. Kozubík, P. Jurdic, K. Soucek and J. Smarda, Growth/differentiation factor-15 inhibits differentiation into osteoclasts—A novel factor involved in control of osteoclast differentiation, *Differentiation*, 2009, **78**(4), 213–222.

41 Y. Qian and X. Chen, ID1, Inhibitor of Differentiation/DNA Binding, Is an Effector of the p53-dependent DNA Damage Response Pathway, *J. Biol. Chem.*, 2008, **283**(33), 22410–22416.

42 T. Iwata, T. Kawamoto, E. Sasabe, K. Miyazaki, K. Fujimoto, M. Noshiro, H. Kurihara and Y. Kato, Effects of over expression of basic helix-loop-helix transcription factor Dec1 on osteogenic and adipogenic differentiation of mesenchymal stem cells, *Eur. J. Cell Biol.*, 2006, **85**(5), 423–431.

43 N. Ferrara, H.-P. Gerber and J. LeCouter, The biology of VEGF and its receptors, *Nat. Med.*, 2003, **9**(6), 669–676.

44 A. Li, S. Dubey, M. L. Varney, B. J. Dave and R. K. Singh, IL-8 Directly Enhanced Endothelial Cell Survival, Proliferation, and Matrix Metalloproteinases Production and Regulated Angiogenesis, *J. Immunol.*, 2003, **170**(6), 3369–3376.

